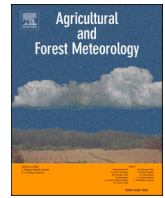




Contents lists available at ScienceDirect

Agricultural and Forest Meteorology

journal homepage: www.elsevier.com/locate/agrformet

Carbon budget response of an agriculturally used fen to different soil moisture conditions

Sonja Paul^{a,b,*}, Christof Ammann^b, Christine Alewell^a, Jens Leifeld^b

^a *Umweltgeowissenschaften, University of Basel, Bernoullistrasse 30, CH-4056 Basel, Switzerland*

^b *Climate and Agriculture Group, Agroscope, Reckenholzstrasse 191, 8046 Zürich, Switzerland*

ABSTRACT

The agricultural use of peatlands usually requires drainage, thereby transforming these organic soils from a net carbon sink into a net source. The Seeland region of Switzerland is characterised by fens that have been intensively used for agriculture for 150 years. Our site is a degraded fen with a remaining peat layer of 60 cm that had been used as cropland until 2009. In connection to a nature protection project it has been managed as extensive permanent grassland since then. The net ecosystem carbon balance (NECB) was determined for two years (2015–2016). For this purpose, the net ecosystem exchange of CO₂ (NEE) and CH₄ fluxes were measured by eddy covariance, and the carbon removed by harvest was quantified. Our degraded fen site was found to be a net carbon source of 477±73 g C m⁻² yr⁻¹ and 434±51 g C m⁻² yr⁻¹ in 2015 and 2016, respectively. Annual CH₄ emissions were marginal in both years with 0.4±0.8 g CH₄-C m⁻² yr⁻¹ (2015) and 0.7±0.7 g CH₄-C m⁻² yr⁻¹ (2016). In contrast to NECB, the NEE was considerably higher in 2015 than in 2016 (308±71 g C m⁻² yr⁻¹ vs 117±39 g C m⁻² yr⁻¹). The year 2015 was characterised by partial flooding of the grassland, followed by a dry and hot summer leading to lower CO₂ uptake due to reduced growth, which was reflected in lower harvest compared to 2016. Thus, the short-term plant-induced carbon fluxes were altered, whereas total soil carbon loss remained rather constant. This was verified by an intra site comparison between the flooded and non-flooded part in 2015. Our results indicate that the soil carbon loss of this highly degraded peatland with a shallow peat layer is relatively moderate and hardly influenced by interannual weather variations.

1. Introduction

Carbon preserved in peatlands constitutes a dynamic reservoir of the global carbon cycle. Over thousands of years partially decomposed organic material accumulates in peatlands due to reduced mineralisation under waterlogged conditions. During peat formation, some carbon is emitted as CH₄ to the atmosphere as a result of anaerobic conditions that allow microbial methanogenesis. Undisturbed peatlands are usually long-term soil C sinks, both in terms of C mass and radiative forcing, (i.e. CO₂ uptake and storage overcompensate CH₄ emission effects) (Frolking et al., 2011). During the last centuries, many peatlands have been drained for agricultural use. The aeration enhances mineralisation, transforming these sites from a net carbon sink into a substantial net source. Globally, drained peatlands emit ca. 1.9 Gt CO₂eq (Leifeld and Menichetti, 2018). In Europe, about 50 % of the peatlands are used for agriculture (Joosten and Clarke, 2002). Consequently, drained peatlands constitute a key greenhouse gas source in many northern European countries (Tiemeyer et al., 2020; Evans et al., 2017; Nielsen et al., 2020). In Switzerland, peatlands cover only 0.68 % of the total surface area, but 600 kt CO₂ are emitted through the use of organic soils, which corresponds to about 10 % of the emissions from the agricultural sector

(FOEN, 2020). Because of their relevance for the climate, studies on greenhouse gas (GHG) fluxes have been emerging and have served as a basis for default annual emission rates (also called 'emission factors', EF) for drained and rewetted organic soils compiled by the Intergovernmental Panel on Climate Change (IPCC) (IPCC, 2014). Based on the main driving factors of GHG emissions from organic soils, the IPCC wetlands supplement has categorized default EFs according to climate zone, land use, soil nutrient status, and drainage status. Uncertainty of the estimates is high, and given the small number of studies, the default EFs are not very robust estimates for specific peatlands. Publication of recent data has further increased the uncertainty: emissions from organic soils in England and Wales either supported the default EFs given by IPCC (2014), or suggested lower emissions for some land use categories (Evans et al. 2017). In contrast, GHG fluxes exceeding the IPCC default EFs by multiple times were measured from grassland and cropland sites in Germany (Tiemeyer et al., 2020). Thus, quantifying the loss of carbon from organic soil remains challenging but is required for the climate reporting under United Nations Framework Convention on Climate Change for each country. Consequently, an enhanced data set is necessary to improve our understanding to develop improved management practices, and to robustly upscale GHG emissions. GHG exchange

* Corresponding author.

E-mail address: sonjamarit.paul@agroscope.admin.ch (S. Paul).

<https://doi.org/10.1016/j.agrformet.2021.108319>

Received 21 August 2020; Received in revised form 18 December 2020; Accepted 31 December 2020

Available online 23 January 2021

0168-1923/© 2021 The Authors. Published by Elsevier B.V. This is an open access article under the CC BY license (<http://creativecommons.org/licenses/by/4.0/>).

measurements of organic soils have yet not been published for Switzerland despite intensive agricultural use (for vegetable cultivation and livestock production) and politically well-connected agricultural subsidies. Further, the carbon loss and soil subsidence are accompanied by increased infrastructure costs for the renewal of drainage and pumping systems. These aspects are crucial to balance the economic yield and ecological costs resulting from the agricultural use of organic soils (Ferré et al., 2019).

Quantification of soil organic carbon change (net carbon sequestration or loss) can be done by measuring all relevant carbon import and export fluxes and integrating the measured net ecosystem carbon balance (NECB) over a full year (Ammann et al., 2007; Aubinet et al., 1999; Leifeld et al., 2011). For peatlands, the NECB is often determined by the net CO₂ exchange with the atmosphere (net ecosystem exchange (NEE)), exchange of CH₄-C, and in the case of managed ecosystems carbon import as organic fertilizers and export as harvest.

The objectives of this paper are: (i) to study the impact of soil moisture and temperature on the net ecosystem carbon balance and its components in two consecutive years for a drained, nutrient-rich managed peat meadow on the Central Swiss Plateau, and (ii) to determine the corresponding CH₄ and CO₂ emission factors.

2. Methods

2.1. Study site

The study site (47°02'37", 7°02'51", 429.3 m NN, Fig. 1 A) was located in the Seeland region, on the Central Swiss Plateau, near the village of Cressier. In this region, fens developed on alluvial or lake sediments after the retreat of the Rhone Glacier in the early postglacial period. The area was first drained in 1864 and agricultural use started in 1920 with arable-ley rotation, including installation of a first subsurface drainage system, which was replaced in 1970. The Cressier site had been under crop rotation before it was converted into an extensively used meadow in 2009. The meadow received no fertilizer and was cut three times a year, with the first cut after 15 June, due to nature conservation regulations. Dominant grass species were *Phleum pratensis*, *Festuca pratensis*, *Poa pratensis* and *Dactylus glomerata*. The grassland was managed by two farmers (eastern and western part) with similar management strategies: in general, grass mowing events occurred on average within 9 days of one another. The water regime was regulated with a drainage and pumping system. Whenever the water table depth was above a specific threshold (0.6 m until 24 March 2016, and 0.5 m afterwards), the pumps started to drain. The site is characterized by a gentle slope from east to west, with a total elevation difference of 0.5 m. The long-term mean annual temperature is 10.2°C and the mean annual precipitation is 957 mm.

To characterise the basic soil properties of the site, 25 soil cores of 4.5 cm diameter and 75-100 cm total depth were sampled in March 2015

with a motor-powered soil corer (HUMAX, CH). The cores were separated into 6-8 layers of 12.5 cm depth, each. Soil samples were dried at 60°C and milled prior to the determination of organic and inorganic carbon (LECO RC612 analyser, USA) and total nitrogen content (LECO CN628 analyser, USA).

The soil of the study site was classified as murshic limnic histosol (WRB, 2014). The humification index according to von Post was between 7 and 10 (Bader et al., 2017; Carter and Gregorich, 2006). The soil was characterised by a shallow peat layer of about 60 cm (Fig. 2), with the upper 30 to 40 cm being highly earthified. This was indicated by low organic carbon content (22 %), relatively low C/N ratio and high bulk density. This layer is underlain by a sapric peat horizon (40-50 cm depth) with carbon contents up to 41 %, a higher C/N ratio of 16. And a lower bulk density of 0.27 g cm⁻³. The carbon stock of the peat layer (incl. only horizons with carbon content > 17 %) was 528 ± 120 t C ha⁻¹ (median ± 2 standard deviations SD). The peat layer was underlain by mineral sediments. The thickness of the different soil layers differs, as indicated by the high variability of carbon content, especially at the lower part of the soil profile.

2.2. Components of the carbon budget

Provided that the soil carbon loss due to erosion or leaching is negligible at the study site, biomass export by harvest (C_{export}) and gaseous carbon exchange as CO₂ (= NEE) and CH₄ are the main processes determining NECB. Thus, it can be expressed as follows:

$$\frac{\Delta SOC}{\Delta t} = NECB = NEE + \text{exchange CH}_4 - C + C_{\text{export}} \quad (1)$$

Note, the gas exchange fluxes follow the micrometeorological sign convention with negative values indicating a net downward flux (i.e. a gain of carbon from the atmosphere). Positive values indicate a loss e.g. carbon export through harvest. Therefore, in Eq. (1) NEE and CH₄ exchange, like the loss term C_{export}, are written with a positive sign. On an annual or longer-term basis, NECB is equivalent to the change of soil carbon storage over time ($\frac{\Delta SOC}{\Delta t}$). Gaseous CO₂ emissions due to mineral weathering represent an additional possible source of CO₂ that is not derived from peat mineralisation (Evans et al., 2016). However, due to the high pH (7.4), little of this flux can be expected to be emitted as CO₂, and therefore to contribute to overall greenhouse gas emissions from the fen (Peacock et al., 2019).

Dissolved organic carbon (DOC) loss was not measured in this study. In most grassland systems, DOC losses contribute only to a minor part to the overall carbon loss. Typical losses of dissolved organic carbon for temperate grasslands are in the order of 5-11 g C m⁻² yr⁻¹ (Evans et al., 2016; Frank et al., 2017; Peacock et al., 2019). This range lies within the lower bounds found for the uncertainty of single component of the carbon budget for our site (Table 1).

For the NECB calculation, all contributing quantities were expressed

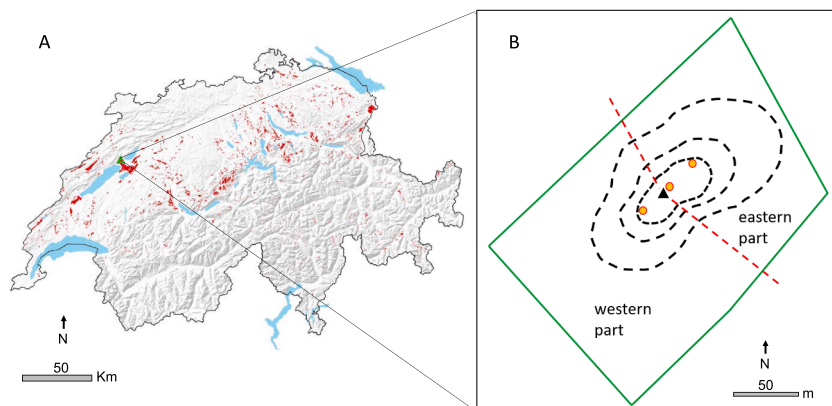


Fig. 1. A) Distribution of organic soil (red area) in Switzerland and location of the measurement site (green triangle; map: FEON/Meteotest, organic soil after Wüst et al. 2015, hillshade and lakes: swisstopo). B) Map of the measurement site with the investigated grassland field (green line), eddy tower (black triangle), groundwater and soil sensor positions (yellow circles). Annual cumulative footprint contributions are indicated by the black dashed contour lines for the contributions of 40, 60, and 80 % (from inside to outwards). The dashed red line indicates the separation of the field into an eastern part, which was flooded in May 2015 and a western part, corresponding to the two main wind direction sectors.

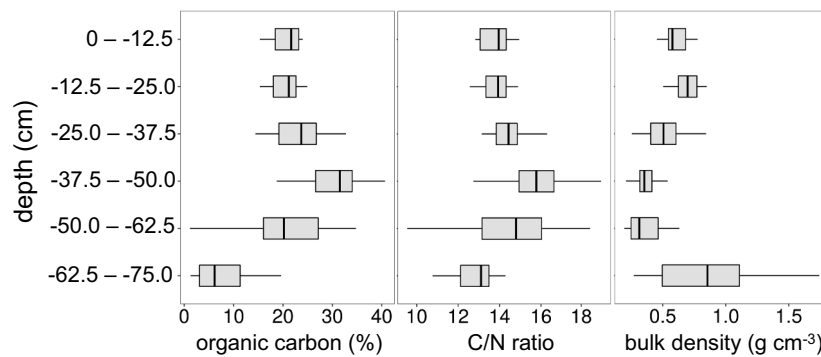


Fig. 2. Organic carbon content, C/N ratio and bulk density for different depth layers (boxplots showing median, 25-75% interval, the highest and lowest value excluding outliers; n=25 soil profiles, data from Lutz, 2016).

Table 1

Uncertainty estimates (95 % confidence interval) for annual NEE (individual error sources and total) harvest yield C_{export} , CH_4 exchange and NECB. All units in $\text{g C m}^{-2} \text{yr}^{-1}$.

	2015	2016
NEE (noise)	28	20
NEE (gaps)	30	11
NEE (u^* threshold)	58	32
NEE (total)	71	39
C_{export}	17	32
CH_4 exchange	0.8	0.7
NECB	73	51

in terms of carbon mass. Yet, for the comparison of the radiative forcing effect of the different greenhouse gases and for the analysis of the net GHG budget, the standard IPCC global warming potentials (GWP_{100}) were used with values of 28 for CH_4 and 265 for N_2O relative to CO_2 , and a time horizon of 100 yr (Myhre et al., 2013). N_2O emissions were estimated from the relationship between soil C/N ratios and N_2O emissions (Leifeld, 2018). Based on the average C/N ratio of 14 (Fig. 2), N_2O emissions of $8.0 \text{ kg N}_2\text{O-N ha}^{-1}\text{yr}^{-1}$ were derived from Leifeld (2018) for our site. This country-specific EF corresponded roughly to the IPCC default EF of $8.2 \text{ kg N}_2\text{O-N ha}^{-1}\text{yr}^{-1}$ (IPCC, 2014). The uncertainty for N_2O emissions was estimated roughly to 100%.

The measurement and the processing of the gas fluxes are described in detail in Sect. 2.4, 2.5, and 2.6. The harvested biomass was determined from the number of hay bales, their average weight, and their dry mass fraction and carbon content. The yield was determined separately for the eastern and western parts of the grassland. The uncertainty of the yield was estimated to 10 % from the error ($2 \times \text{SE}$) in weighing the hay bales (Ammann et al., 2007).

2.3. Meteorological and soil measurements

Meteorological parameters were continuously monitored close to the EC tower. Air temperature, pressure, relative humidity, and precipitation were measured with a Vaisala Weather Transmitter (WXT520, Finland). Global radiation was measured with a Pyranometer Sensor (SKL 2655, Skye Instruments Ltd, UK). The devices were mounted at the same height as the EC system. Data were measured at 0.1 Hz and average values were logged every 10 min on a CR1000 (Campbell Scientific, UK). Data gaps (01.01.-07.01.2015 and 13.09.-06.10.2016) of the weather parameters were filled with data from a nearby meteorological station (Cressier, 1 km distance, same altitude) of the Swiss national observation network (operated by MeteoSwiss, the Federal Office of Meteorology and Climatology).

Soil water content and soil temperature were measured (in one minute intervals) in three profiles with a soil moisture sensor (GS3 and

5TE decagon devices, NE Hopkins Court, USA). The averages were logged every 30 min on EM50 digital loggers (decagon devices, NE Hopkins Court, USA). Since February 2015, a soil profile (n=2 for 5 cm depth; n=1 for the other sampling depth: 10, 20 and 40 cm) was measured near the EC system. In November 2015, two additional soil profiles with identical setups were installed in the main footprint areas to better cover the spatial heterogeneity.

Three groundwater observation wells were installed in August 2015 (Fig. 3). At two sites (near the EC tower and at the eastern part) the groundwater level was measured continuously and logged every 30 minutes with a pressure probe (CTD/CTD-GPRS, UIT, Umwelt- und Ingenieurtechnik GmbH Dresden, Germany). The third groundwater observation site (located in the western part) was measured manually with an electrical contact gauge about every 2-4 weeks. Missing groundwater table data from February 2015 to August 2015 were modelled based on a fitted non-linear regression between the measured soil water content and groundwater table data from August 2015 to September 2016 ($r^2 = 0.83$; $\text{RMSE} = 0.09 \text{ m}$). From August 2015 onwards, missing groundwater data – due to a failure in a single measurement device – were replaced using linear regression between the individual groundwater measurements. They generally showed a high temporal correlation of $r^2 = 0.97$ ($\text{RMSE} = 0.05 \text{ m}$).

2.4. Gas flux measurements

The net exchange of CO_2 and CH_4 between the ecosystem and atmosphere was measured using the eddy covariance (EC) method near the centre of the meadow field (Fig. 1 B). A three-dimensional sonic anemometer (CSAT-3, Campbell Scientific, UK) was used to measure directional wind velocities and temperature. Fast-response open-path infrared gas analysers were used for measurements of CO_2 (non-dispersive infrared spectroscopy, LI-7500A, LI-COR Biosciences, USA) and CH_4 (wavelength modulation spectroscopy, LI-7700, LI-COR Biosciences, USA). The EC system was installed on a tripod tower 2.0 m above canopy height. The height of the EC system above ground was adjusted regularly to account for the height of the growing vegetation. Typically, the height of the EC system varied between 2.2 m and 2.6 m above ground, and data were recorded with a frequency of 10 Hz on the LI-7500a system. The zero and the span of the CO_2 analyser were set using high-purity N_2 zero gas and one standard gas with concentrations of 495 ppm for CO_2 and 1.92 ppm for CH_4 . Standard gases with lower concentrations of 346 ppm (CO_2) and 1.45 ppm (CH_4) were used to check the performance and linearity of the calibration. The operating temperature of the gas analysers was changed in spring and in fall (to summer and winter mode, respectively) to avoid internal heating effects, with the temperature changes being accompanied by a calibration.

Due to a breakdown of the LI7500A (23.11.2015-20.01.2016), an alternative system was used to measure CO_2 and H_2O fluxes (23.12.2015 to 20.01.2016) consisting of a LI7500 (LI-COR Biosciences, Lincoln,

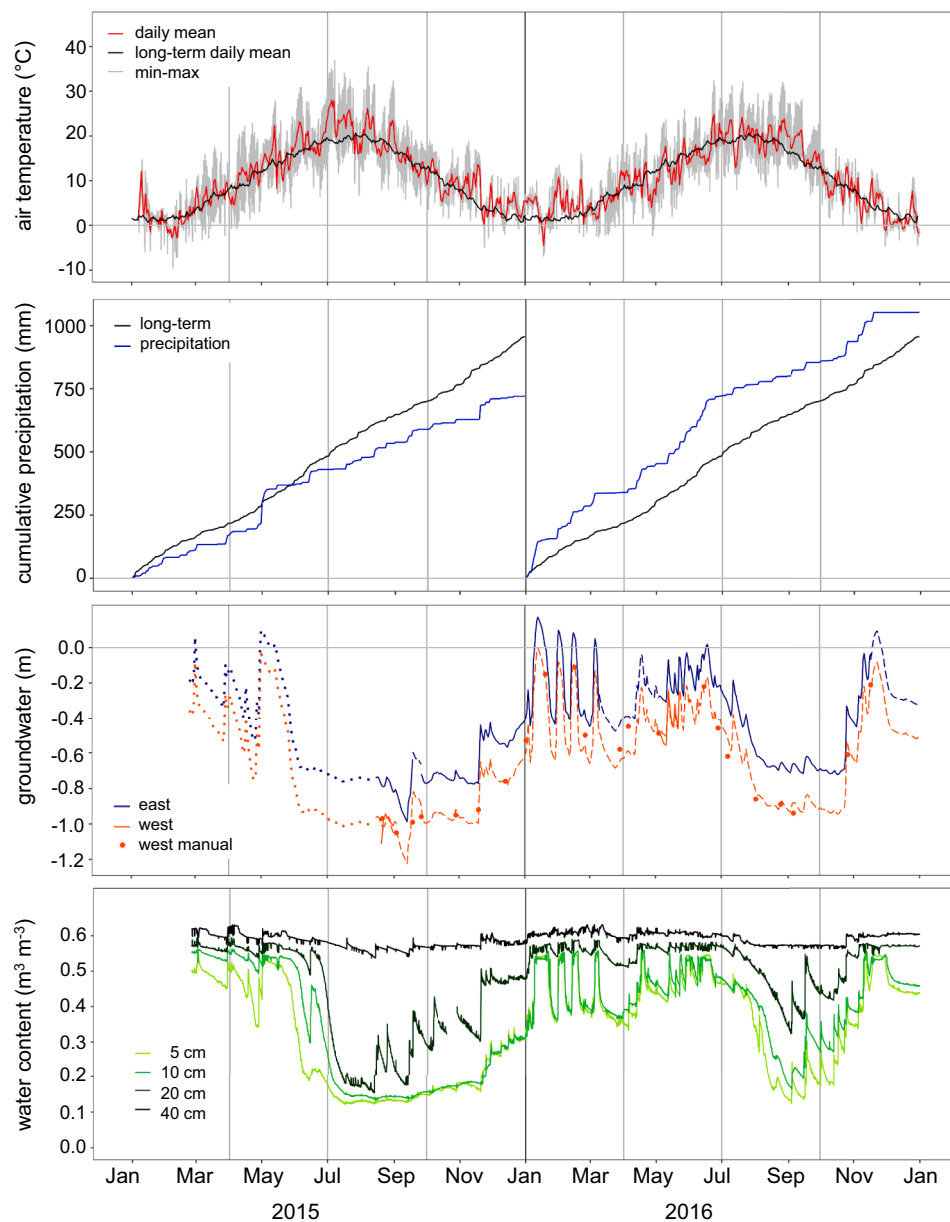


Fig. 3. Daily mean air temperature and temperature range (min - max) measured at about 2 m above canopy height and cumulative daily precipitation at the study site for the years 2015 and 2016. For comparison, the long-term average at the meteorological station Cressier is shown as black line (data from 2010-2018 for precipitation and 1992-2018 for air temperature). Groundwater tables of the observations wells from the eastern and western part (dotted line: modelled data; solid line: measured data) and soil water content of four soil depths measured at the tower.

USA). Data were logged on a CR1000 (Campbell Scientific UK). No CH_4 data were measured from 23.12.2015 to 20.01.2016 as the LI7700 was not integrated to the alternative EC-system.

2.5. Flux calculation and quality control

Half-hourly mean CO_2 and CH_4 fluxes were calculated from high-frequency data using the EC software EddyPro® (Version 6.2.1; 2016), using the widely adopted 2-D wind vector rotation and linear detrending (Vickers and Mahrt, 1997; Gash and Culf, 1996). Air density fluctuations were compensated according to Webb et al. (1980). Time lags were compensated using the covariance maximization with the default method. A statistical test for raw data screening was done after Vickers and Mahrt (1997). To correct flux estimates for low and high-frequency losses due to the instrument setup and intrinsic sampling limits of the instruments, the methods according to Moncrieff et al. (1997) and Moncrieff et al. (2004) was used. The footprint estimation was implemented according to Kormann and Meixner (2001).

Temperature-dependant CSAT-3 offsets were identified and

corrected separately for winter time (01.10.-15.04.) with $u: 0.16 \text{ m s}^{-1}$, $v=-0.03 \text{ m s}^{-1}$ w: 0.01 m s^{-1} and summertime (15.04.-01.10.) with $u: 0.2 \text{ m s}^{-1}$, $v=-0.45 \text{ m s}^{-1}$ w: 0.05 m s^{-1} . Calculated fluxes were quality flagged for micrometeorological tests (Mauder and Foken, 2011). Flag values were 0 (best quality), 1 (suitable for annual budgets) and 2 (bad quality). CO_2 fluxes were removed when: (a) their quality flag was >1 ; (b) the signal strength was $<95\%$ (Li7500A) or the AGC value was $>75\%$ (Li7500); (c) CO_2 concentration was >800 ppm; (d) the rotation angle for tilt correction was $< -3^\circ$ or $> 4^\circ$; (e) u^* was $< 0.065 \text{ m s}^{-1}$ as determined by the MPI-Jena online gap-filling tool; and (f) time lag for CO_2 was $<-0.7 \text{ s}$ or $>0.7 \text{ s}$. In addition, based on the relationship between T_{soil} and NEE measured at night, a temperature-dependent threshold for implausible high positive (or negative) CO_2 fluxes was used to remove outliers. It eliminated only 0.3 % (2015) and 0.6 % (2016) of the total dataset. The entire quality filtering process and the loss of data due to malfunction of the EC system led to a data coverage of 42 % for 2015 and 44 % for 2016 of the entire CO_2 data set.

CH_4 fluxes were removed when: (a) the signal strength was $<40\%$; (b) their quality flag was > 1 ; (c) the rotation angle for tilt correction

pitch < -3° or $> 4^\circ$; (d) $u^* < 0.065 \text{ m s}^{-1}$, was determined by the MPI-Jena online gap-filling tool; and (f) time lag for CH_4 was $< -1.1 \text{ s}$ or $> 1.1 \text{ s}$. For CH_4 , the total data coverage was 42 % in 2015 and to 39 % in 2016.

The gas exchange and carbon budget of the site was evaluated for the entire grassland site including all wind directions. Additionally, we separated the site into an eastern and a western part (Fig. 2), reflecting the two main wind sectors. Slightly lower elevation and a higher groundwater table characterize the eastern part. To analyse the sensitivity of this elevation effect on the carbon cycling, we followed the approach of Wall et al. (2020) and used our single EC system to calculate the NEE and NECB separately for the two adjacent sectors. The NEE time series was separated accounting for the wind direction into a (north-) easterly sector ($> 330^\circ$ or $< 140^\circ$) and in a (south-)westerly sector ($> 140^\circ$ or $< 330^\circ$). For some periods with very low nighttime data coverage ($< 5\%$ for two out of three weeks), a separation was not meaningful and data from all wind directions were used. This occurred only in the second half of the year and in January 2016. The total annual data coverage of western and eastern sector was 16 % and 27 %, respectively.

2.6. Flux gap-filling and uncertainty estimation of annual sums

To obtain annual NEE budgets, data gaps for CO_2 fluxes were filled using the New ReddyProcWeb online tool, developed at the Max Planck Institute for Biogeochemistry, Jena, Germany (Reichstein et al., 2005; Wutzler et al., 2018). To partition the measured NEE into gross primary production (GPP) and ecosystem respiration (Reco), the nighttime partitioning approach was used (Reichstein et al., 2005). Briefly, it is assumed that the temperature response function of nighttime NEE fluxes is also applicable for daytime data. Daytime Reco is then predicted from the measured soil temperature, while GPP is calculated as the difference between NEE and Reco. The environmental factors used for the gap-filling were: global radiation, soil temperature at 5 cm depth, vapour pressure deficit, and friction velocity (u^*). Filling of gaps was performed based on similar meteorological conditions using a lookup table. The time window in which the method was looking for similar results was seven days, in absence of similar conditions, the window was extended to 14 days.

For CH_4 fluxes by the open path Li7700 LICOR device, no systematic dependence on potential driving factors and no diurnal cycle were found. Therefore, monthly average fluxes were directly calculated from the quality filtered dataset. The annual CH_4 budget was determined as sum of the monthly fluxes and its uncertainty was estimated as $2 \times \text{SE}$ (determined from the variability of monthly data) for the two individual years. This uncertainty represents an upper limit because it may also include systematic seasonal variations. The flux detection limit for CH_4 fluxes measured with the open path Li7700 LICOR device was estimated to be approximately $3 \pm 3 \text{ nmol m}^{-2} \text{ s}^{-1}$ ($3 \text{ mg CH}_4\text{-C d}^{-1}$; Deventer et al., 2019).

Annual NEE values are associated with different kinds of random-like and systematic uncertainties (Goulden et al., 1996). In this study, three components of NEE uncertainties were considered and computed (as $2 \times \text{SD}$) separately:

- i) The random uncertainty was assessed by adding additional noise to the measured NEE data before gap-filling (Felber et al., 2016). The random error of individual fluxes was estimated as the standard deviation of the residuals between measured NEE fluxes and inferred fluxes by the gap filling routine (assuming a gap at the place of the valid measured flux). Linear regressions for SD vs NEE were applied to bins of $2 \mu\text{mol m}^{-2} \text{ s}^{-1}$ width and separately for positive and negative NEE values (Felber et al., 2016; Jérôme et al., 2014).

The following regression parameters were found for the NEE dataset:

$$\text{SD} = 0.0626 \text{ NEE} + 1.499 \text{ for NEE} > 0 \text{ (R}^2 = 0.87)$$

$$\text{SD} = -0.1013 \text{ NEE} + 1.570 \text{ for NEE} \leq 0 \text{ (R}^2 = 0.89)$$

These parametrisations were used to add additional noise to the measured NEE assuming a normal distribution. We performed ten simulation runs with subsequent gap-filling.

- ii) The uncertainty due to larger gaps was estimated by adding artificial gaps to the existing dataset. The five largest gaps of 2016 were inserted in the 2015 dataset and vice versa. Moreover, these additional gaps were shifted in several steps between -720 and $+720$ hours resulting in 11 datasets with varying gap patterns for each year. The resulting uncertainty was estimated from the $2 \times \text{SD}$ of the 11 annual NEE data sets with the additional artificial gaps for each year.
- iii) The systematic uncertainty of u^* filtering was determined by varying the u^* threshold prior to gap-filling within a range of -0.04 and $+0.06 \text{ m s}^{-1}$ around the chosen threshold 0.065 m s^{-1} . We then calculated the standard deviation of the resulting six annual NEE datasets.

The total uncertainty for NEE and NECB was subsequently calculated by combining the individual uncertainties using Gaussian error propagation (Felber et al. 2016, Table 1).

3. Results

3.1. Environmental conditions and grassland harvests

In the first year (2015), the study site Cressier received 720 mm annual precipitation, a quarter less than the long-term annual precipitation average (Fig. 3). In May, an exceptionally heavy rain event occurred and the following summer was extraordinarily hot: average maximum air temperature in June to July was 29.5°C (min-max: $19.9\text{--}37.5^\circ\text{C}$; SD 4.7°C) in 2015, while the temperature was about 3.4°C cooler for the same period in 2016. The year 2016 was characterized by a relatively cold spring and early summer, followed by a very humid June, leading to relatively high groundwater tables (Fig. 3). The average groundwater table was lower in 2015 (-0.60 m) than in 2016 (-0.44 m), but fluctuated strongly throughout the seasons (min: -1.20 m ; max: 0.11 m). High water tables were measured in winter and spring seasons. In May 2015, a heavy rain event lead to partially flooding of the eastern part for about three weeks (Fig. 3 and field observation). The following summer was characterized by a prolonged period of low water table (-0.8 m from June to December 2015). In contrast, in summer 2016 the groundwater table was at a depth of -0.6 m for only 3 months (August–October 2016). The groundwater table on the east side was generally higher (on average by 0.21 m) with a few flooding episodes in Mai 2015 and the beginning of 2016 than on the west side, which reflects the topographic differences, i.e. the slight slope of the study site. We observed that the soil water content and groundwater table closely followed rain events (Fig. 3). The dry summer conditions of 2015 are also reflected in very low water content in the upper soil ($< 0.2 \text{ m}^3 \text{ m}^{-3}$, Fig. 3) during July to November 2015 (5, 10 and 20 cm). In contrast, these soil layers were relatively moist in June and July in 2016 and lower soil water contents were only observed from August to October of that year.

In 2015, the total yield of the three cuts was 169 g C m^{-2} , which was about half of 2016 (Table 2). In 2015, the yield of the first cut was smaller in the eastern, partly flooded part of the grassland, while in 2016, yields of the two parts of the grassland were similar.

3.2. Gas fluxes and carbon budget

3.2.1. CO_2

We found pronounced diurnal and seasonal variations in half-hourly NEE values during both measurement years (Fig. 4). Negative values usually represent daylight fluxes dominated by CO_2 uptake. Each

Table 2
Mowing dates and carbon removal by harvest (in units g C m^{-2}).

	cut	East part mowing date	East part harvest	West part mowing date	West part harvest	Entire field harvest
2015	1 st	19.06.2015	72	23.06.2015	140	106
	2 nd	12.08.2015	31	07.08.2015	35	33
	3 rd	09.10.2015	27	22.10.2015	32	30
	Total		130		208	169
2016	1 st	26.06.2016	226	01.07.2016	197	212
	2 nd	22.08.2016	54	24.08.2016	65	59
	3 rd	03.10.2016	49	29.10.2016	42	46
	Total		329		304	317

mowing event was followed by a sharp reduction of CO_2 uptake and a subsequent steady increase in magnitude. However, in May 2015 a reduction of CO_2 uptake also occurred few days after the flooding event. In addition, the average daylight NEE between the first and second cut was considerably less negative in 2015 than in the following year ($-1.2 \mu\text{mol mol}^{-1}$ vs $-3.0 \mu\text{mol mol}^{-1}$). Both study years showed a positive cumulative NEE of $308 \pm 71 \text{ g C m}^{-2} \text{ yr}^{-1}$ in 2015 and $117 \pm 39 \text{ g C m}^{-2} \text{ yr}^{-1}$ in 2016, respectively (Fig. 5). Reduced carbon uptake from May to June 2015 and from July to mid August 2015 compared to 2016 resulted in a higher positive NEE in 2015 (Figs 4, 5). The same pattern is observed for both sectors of the grassland: from May onwards the net cumulative NEE of the eastern (flooded) part increased only slightly, while we observed a distinct carbon uptake for the (non-flooded) western sector until mid-May, followed by a rather constant net cumulative NEE until mid-June. Thus, the NEE of the western part was slightly lower compared to the eastern part ($273 \text{ g C m}^{-2} \text{ yr}^{-1}$ vs $341 \text{ g C m}^{-2} \text{ yr}^{-1}$). In contrast, the period of net carbon uptake was substantially longer in 2016 (8.3. - 22.06.2016). Further, no difference in annual NEE was observed between the eastern and western part. In 2015, the GPP was $1620 \pm 49 \text{ g C m}^{-2} \text{ yr}^{-1}$ and considerably lower than in 2016 ($1930 \pm 56 \text{ g C m}^{-2} \text{ yr}^{-1}$), while Reco was rather similar in both years ($1928 \pm 88 \text{ g C m}^{-2} \text{ yr}^{-1}$ and $2046 \pm 80 \text{ g C m}^{-2} \text{ yr}^{-1}$, respectively).

3.2.2. CH_4

Annual CH_4 emissions were $0.4 \pm 0.8 \text{ g CH}_4\text{-C m}^{-2} \text{ yr}^{-1}$ (2015) and $0.7 \pm 0.7 \text{ g CH}_4\text{-C m}^{-2} \text{ yr}^{-1}$ (2016) and thus marginal in comparison to annual NEE. Slightly higher emissions were measured in spring 2015 (Fig. 6). The eastern part of the field, which was flooded in May 2015, emitted on average $2.9 \text{ mg CH}_4\text{-C m}^{-2} \text{ d}^{-1}$ in May 2015. After 16 days of flooding, the highest daily CH_4 emissions of $13.4 \text{ CH}_4\text{-C m}^{-2} \text{ d}^{-1}$ were measured (Fig. 7), followed by decreasing emissions corresponding with drying of the grassland. The following three months were characterized by low emissions in both parts, accompanied by a small CH_4 uptake.

3.2.3. Net ecosystem carbon balance

The individual components of the carbon budget differed

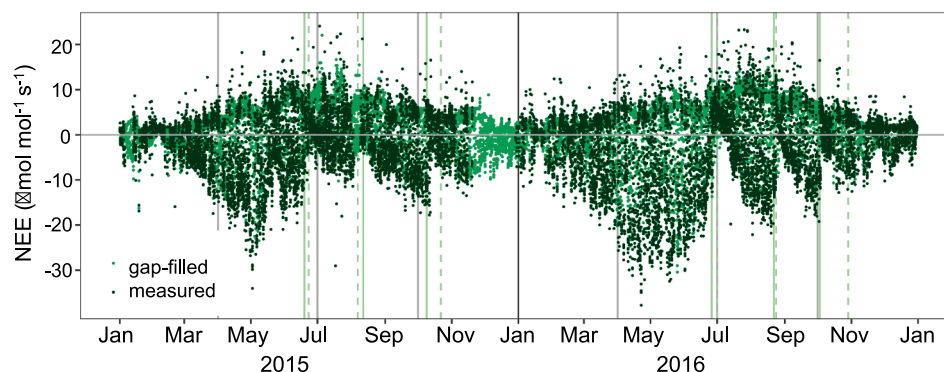


Fig. 4. Measured and gap-filled half-hourly CO_2 fluxes in 2015 and in 2016. Green lines represent mowing dates (solid: eastern part, dashed western part).

considerably between 2015 and 2016, but also between the eastern (flooded) and western part in 2015. However, the resulting annual NECB was very similar for both years ($477 \pm 73 \text{ g C m}^{-2} \text{ yr}^{-1}$ in 2015, and $434 \pm 51 \text{ g C m}^{-2} \text{ yr}^{-1}$ in 2016) (Fig. 8). The higher NEE in 2015 was compensated by a low harvest, leading to similar net carbon loss as the 2016 budget. In 2015, the NECB was $471 \text{ g C m}^{-2} \text{ yr}^{-1}$ in the eastern (flooded) part and $481 \text{ g C m}^{-2} \text{ yr}^{-1}$ in the western part. The reduced harvest in combination with higher NEE of the eastern (flooded) part offset the differences in net carbon balance in 2015 for both sectors. Compared to CO_2 fluxes, CH_4 fluxes were negligible.

4. Discussion

4.1. CH_4 fluxes

The relatively low annual CH_4 emission rates of this well-drained site are in line with other intensively used organic soils (Poyda et al., 2016; Tiemeyer et al., 2016). The main driving factor of CH_4 emissions is the groundwater level. In agreement with this, low average CH_4 emissions of $0.02 \pm 0.35 \text{ g CH}_4\text{-C m}^{-2} \text{ yr}^{-1}$ were measured in 20 deeply-drained fens in Germany, compared to higher emissions of $7.98 \pm 10.4 \text{ g CH}_4\text{-C m}^{-2} \text{ yr}^{-1}$ for shallow-drained nutrient-rich German peatlands (Tiemeyer et al. 2016). Generally, a drainage depth of -0.25 m is sufficient to inhibit the diffusion of high amounts of CH_4 into the atmosphere, as CH_4 produced in the anoxic zone is oxidized by methanotrophs in the oxic zone (Jungkunst et al., 2008; Turetsky et al., 2014). In addition, our site lacks aerenchyma shunt species, which enable CH_4 transport from the anaerobic layer to the atmosphere, bypassing the oxic zone and thus increasing CH_4 emissions (Whiting and Chanton, 1992).

Although the water table at our site is dynamic and includes periods where the water table is clearly above -0.2 m , CH_4 emissions remained

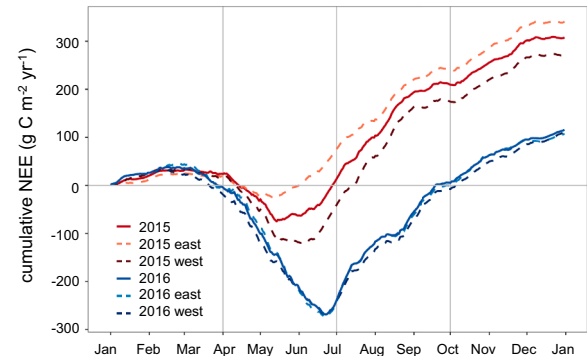


Fig. 5. Cumulative net ecosystem exchange (NEE) over the years 2015 and 2016, for the whole grassland and separately for the eastern and the western part of the grassland.

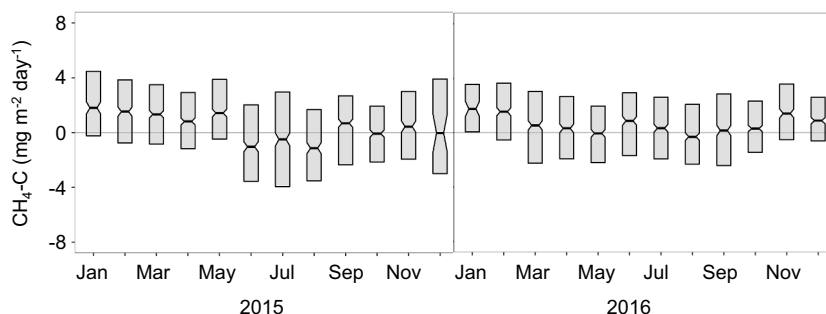


Fig. 6. Daily CH₄ fluxes (boxplots showing median and 25% and 75% quantile) of the grassland in 2015 and 2016.

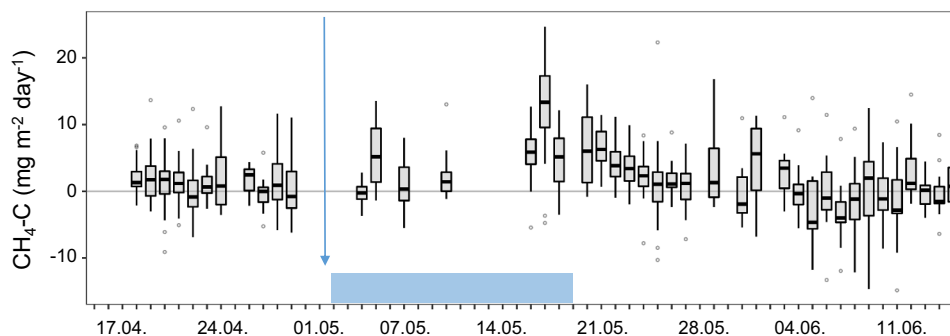


Fig. 7. Daily CH₄ fluxes of the eastern part of the grassland field from 15.4.-15.6.2015 (boxplots showing median, 25% and 75% quantile, the highest and lowest value excluding outliers, and potential outliers as points, boxplots are shown if the number of half-hourly fluxes per day were >3). The blue arrow indicates the heavy rain event and the subsequent flooding period (blue region).

rather low throughout the year. Recent studies found that the summer groundwater level (rather than annually-averaged groundwater levels) was the main driving factor of CH₄ emissions (Renou-Wilson et al., 2016; Tiemeyer et al., 2016). Accordingly, the relatively high water table in winter and spring left no imprint in the CH₄ emissions at our site. Lowest CH₄ emissions and even net uptake were observed during summertime with very low soil water content in 2015, supporting general findings of reduced CH₄ emission or even uptake by drained organic soils (Maljanen et al., 2010). CH₄ uptake is characteristic for oxic mineral soils and was found to vary from -0.01 to -0.68 g CH₄-C m⁻² yr⁻¹ (mean -0.12) in northern Europe (Smith et al., 2000).

Short periods of high groundwater table, including flooding in May 2015 and June 2016, did not lead to substantial CH₄ emissions for the whole grassland. However, after 17 days of flooding in May 2015 in the eastern part of the grassland, CH₄ emissions increased slightly up to 13.4 g CH₄-C m⁻² yr⁻¹. This is in agreement with incubation experiments where peat soils were flooded after an artificial drought. CH₄ emissions were reduced for days to weeks after rewetting (Knorr et al., 2008). After 17 days of flooding at our site, we observed a partial die-off for the wetness-intolerant plants such as *Lolium*. We assume that this plant material may serve as an easily degradable carbon source needed for high CH₄ emissions, as it was shown in incubation experiments (Hahn-Schöfl et al., 2011). However, due to the pumping system at our site, the ground water level decreased and consequently terminated the phase of anaerobic soil conditions. Apparently, the period where the water table was elevated was too short at our site to establish substantial methanogen-driven anaerobic decomposition of plant debris. Although degraded peatlands are prone to flooding conditions after heavy rain events, due to the hydrophobic properties of degraded peat, and compacted soil horizons, substantial CH₄ emissions might not occur as long as flooding periods are restricted to two weeks.

4.2. NECB and GHG budget

The soil carbon loss for the site was 477±73 g C m⁻² yr⁻¹ in 2015 and 434±51 g C m⁻² yr⁻¹ in 2016 and thus within the lower bounds found for deep-drained temperate organic grassland soils (Tiemeyer et al., 2016; IPCC, 2014). Recent publications demonstrate the high variability of emission rates: Tiemeyer et al. (2016) analysed a comprehensive dataset consisting of 48 German grasslands on organic soils. The mean soil carbon loss for 20 deep-drained nutrient-rich grasslands was 960±530 g C m⁻² yr⁻¹; considerably higher than the IPCC default EF of 610 g C m⁻² yr⁻¹. Besides the ground water level, a complex interaction of soil properties, hydro-meteorological conditions, plant communities, and ecosystem management affects the loss of soil carbon. Fertilisation - and thus intensive management - likely corresponds with increased CO₂ emissions. For example, most of the grassland analysed by Tiemeyer et al. (2016) with emissions exceeding the IPCC default EF were fertilised. This finding is supported by the generally lower soil carbon loss found for nutrient-poor peatlands (IPCC 2014, Tiemeyer et al. 2016). Moreover, incubation experiments showed that nutrient status, especially potassium and phosphorus availability, increases mineralisation rates in peatland soils (Säurich et al., 2019; Sundström et al., 2000). Thus, the extensive use of our meadow (no fertilisation and first cut only after mid-June) could be one factor for the relatively low NECB.

Besides the extensive use of our grassland, the long-lasting aerobic conditions and the resulting change in soil organic matter quality may have had an impact on the soil carbon loss rates at the Cressier site. During decomposition, peat is depleted in easily degradable polysaccharides, and more recalcitrant fractions accumulate within the profile (Leifeld et al., 2012; Sangok et al., 2017; Sjögersten et al., 2016). The content of O-alkyl-C served as an indicator for the duration of aerobic decomposition processes: with the duration of aerobic exposure, O-alkyl-C decreased concurrently with emission rates (Leifeld et al. 2012). The finding that poorly decomposed peat emits more CO₂ than strongly decomposed peat was confirmed by others in incubation

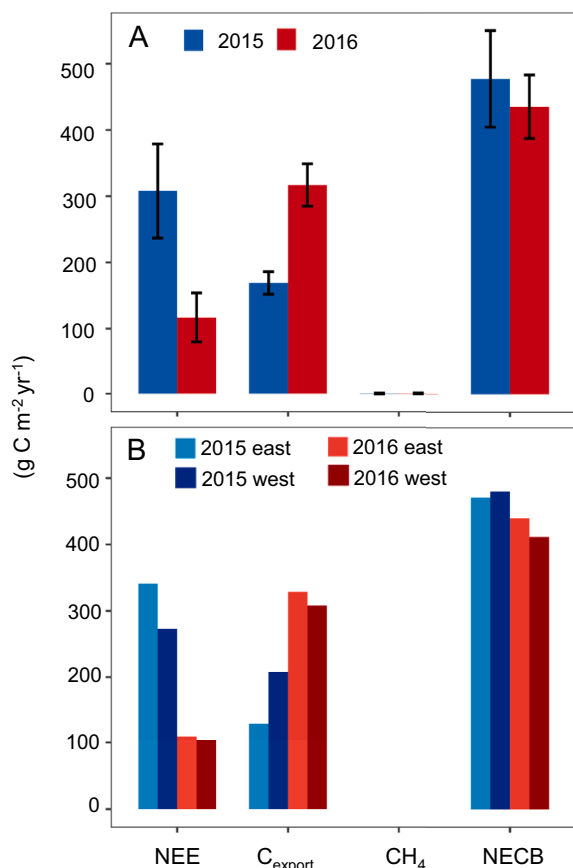


Fig. 8. Carbon budget components for (A) the whole grassland and for (B) the eastern (flooded in May 2015) and western sectors.

experiments (Glatzel et al., 2006). Our site has had subsurface drainage and was tilled for nearly 100 years. Moreover, most of the remaining peat layer has generally remained above the average groundwater level during the growing season. Thus, a substantial portion of the peat was exposed to aerobic mineralization for decades. Indeed, highly degraded peat, with high contributions of aromatic compounds, was indicated by low O/C and H/C ratios at the Cressier site (Bader et al., 2017; Visser, 1983). Relatively narrow C/N ratios through the entire profile also indicates highly decomposed organic matter at the Cressier site, as during decomposition C is preferentially lost over N (Krüger et al., 2015; Kuhry and Vitt, 1996). In addition, relatively low emission rates were found in incubation experiments of 21 drained organic soils from Switzerland, compared to undisturbed and extensively managed organic soils (Bader et al., 2018). More specifically, incubation experiments of top- and subsoils from the Cressier site showed similar mineralization rates for the different depths (Bader et al., 2018). The authors attributed the relatively high stability of carbon in the upper soil horizon to the highly recalcitrant organic matter due to the previous intense decomposition processes stimulated by drainage and decades-long agricultural use. Thus, our relatively low observed emission rates might be also attributed to the relative stability of the already highly decomposed peat material.

Despite the contrasting weather conditions, the loss of soil organic carbon was rather similar for the last two years. Tiemeyer et al. (2016) showed a peatland-specific CO₂ response to groundwater fluctuations. However, changes in soil moisture did not affect the annual soil carbon loss at our site. One explanation might be that the differences in soil moisture in 2015 resulted in a net zero effect in the C budget. The wet period during May 2015 might have been too short to reduce mineralisation rates sufficiently to be reflected in the annual carbon budget. Indeed, reduced respiration was only observed for one (eastern part) to

three weeks (western part, data not shown). Also, Han et al. (2014) observed a reduction in nighttime respiration after a flooding event, but the effect was visible for only 10 days after flooding in that field experiment.

Similarly, the carbon loss on an annual basis was not influenced by the drier soil conditions in 2015 during summertime. Due to the shallow peat layer (0.6 m depth) at the Cressier site, no additional peat material was exposed to oxygen in 2015, when the groundwater level fell up to 1.2 m in the summer of that year. This may explain the absence of increased organic carbon mineralization. Moreover, the effect of drier soil conditions in the deeper peat layer, which could result in increased mineralisation, might be offset by very dry soil conditions in the upper peat layer leading to reduced mineralisation. This was also confirmed in laboratory incubations of peat soils showing that respiration was limited by very low moisture levels (Glatzel et al., 2006; Säurich et al., 2019; Toberman et al., 2008). In agreement with this, the highest CO₂ emissions occurred at deeply drained sites that had highly dynamic groundwater levels and lacked drought stress (Tiemeyer et al., 2016).

Another explanation might be that highly degraded and recalcitrant peat under intensive use is less sensitive to alteration in soil moisture. Poyda et al. (2016) observed constant emission rates of 1300 g C m⁻² yr⁻¹ for an intensively-used, degraded grassland for two consecutive years, while a nearby extensively used, shallow-drained grassland emitted 700 g C m⁻² yr⁻¹ and 1300 g C m⁻² yr⁻¹ in the same years. High interannual variability of NECB varying from 143 to 880 g C m⁻² yr⁻¹ (mean: 210±250 g C m⁻² yr⁻¹) in four consecutive years was also reported for drained grasslands on deep fen peat in NW Germany (Beyer et al., 2015). However, the lack of long-term time series data makes it difficult to determine whether highly degraded peatlands with shallow peat layers indeed show less inter-annual variability compared to more undisturbed peatlands.

The GHG budget was dominated by CO₂ fluxes: the marginal CH₄ emissions of 0.15±0.30 and 0.26±0.26 t CO₂eq ha⁻¹ yr⁻¹ did not contribute to the total GHG emissions. The estimated N₂O emissions were 3.3±3.3 t CO₂eq ha⁻¹ yr⁻¹. Accounting for all GHG-fluxes – including the estimation for N₂O – the GHG budget resulting in 20.9±4.3 (2015) and 19.5±3.8 t CO₂eq ha⁻¹ yr⁻¹ (2016), quite similar for both years.

4.3. Components of NECB

Even though the NECB was relatively similar in the two consecutive years, the individual components of the NECB were sensitive to changing weather conditions. A short period of flooding in May 2015 led to reduced NEE during spring and early summer compared to 2016. This was considered to be due not to reduced degradation of soil organic matter, but rather to reduced photosynthesis of plants. The most important constraint for plants during flooding is oxygen deficiency (Vartapetian and Jackson, 1997). As a consequence, growth rate and biomass production of terrestrial plants are reduced under flooded conditions (Gibberd, 2001; van Eck et al., 2004; Wright et al., 2017). Thus, high rainfall conditions at our site led to unfavourable growth conditions for the grass vegetation that was not well-adapted to saturated soil conditions (e.g. as they lack the aerenchyma systems of many wetland plants). Reduced plant biomass production was reflected by a reduction in yield by 50 % in 2015 for the first cut compared to 2016. The same holds for the two sectors of the grassland in 2015. In the eastern part of the meadow, which was partly flooded in May 2015, CO₂ uptake was further reduced, mirrored by a lower harvest compared to the western site, which was unaffected by the flooding.

The growth conditions at the Cressier site remained rather unfavourable in 2015, as a dry and hot summer followed, causing very low soil moisture content combined with high air temperatures. Water stress limits plant growth through diminished leaf C fixation resulting from stomatal closure to reduce transpiration (Signarbieux and Feller, 2012). High temperatures lead to reduced photosynthesis through thermal

damage in plants (Allakhverdiev et al., 2008). Generally, the combination of drought and heat stress results in a decrease in gross primary production, which could be observed in the extraordinarily dry and hot summer in Europe in 2003 (Reichstein et al., 2007; von Buttlar et al., 2018). In Switzerland, it was estimated that the 2003 heatwave caused a 20–30 % reduction in grassland production (Keller and Fuhrer 2004). Thus, the 50 % lower yield for the second cut in 2015 compared to the following year may be explained by reduced photosynthesis due to the combination of water and temperature stress.

However, the impact of drought on the components of NECB in peatlands differs considerably depending on peat type, vegetation and degradation status. Generally, mineralization of peat increases in dry years, as the lower water table exposes more soil organic matter to oxygen. In contrast, the response of plants to drier soil conditions strongly depends on vegetation types and characteristic of drought. In near-natural peatlands, wetland-adapted vegetation such as sedges or sphagnum mosses show a strong reduction in CO₂ uptake in dry years, turning these peatlands from carbon sinks to carbon sources (Alm et al., 1999; Bubier et al., 2003a; Griffis et al., 2000; Lafleur et al., 2003). In only slightly disturbed peatlands, or within the drier sites of natural peatlands, (such as hummocks), vegetation adapted to drier soil conditions. These vegetation types responded to the drier soil conditions with enhanced carbon uptake (Bubier et al., 2003b; Drollinger et al., 2019; Flanagan and Syed, 2011). The combination of simultaneous increased mineralisation and CO₂ uptake rates can turn these peatlands into carbon sources (Bubier et al., 2003a; Cai et al., 2010; Lafleur et al., 2003) or to carbon neutrality (Drollinger et al., 2019). Moreover, areas with deciduous trees were found to represent a net carbon sink in a dry year, as the increased GPP overcompensated for the increased ecosystem respiration (Bubier et al., 2003a). However, in a temperate peatland affected by past agricultural activities, drainage and mining, a severe drought led to reduced GPP of the grassland vegetation and to increased mineralization (Aslan-Sungur et al., 2016). This resulted in a threefold increase in CO₂ source strength compared to other years during a four-year measurement campaign (Aslan-Sungur et al., 2016).

In contrast, at our agriculturally-used fen, respiration was similar in both years. We observed substantially lower GPP in the dry year compared to 2016 (1620 vs 1930 g C m⁻²yr⁻¹) for the entire grassland. In 2016, under more favourable growth conditions, the considerably higher yield was counterbalanced by higher NEE. Thus the overall NECB and soil carbon loss were rather unaffected by environmental conditions.

5. Conclusion

While the individual components of NECB, mainly NEE and C export by harvest, reacted sensitively to different soil moisture conditions in the study years, the resulting annual NECB values were not significantly different. A flooding event in May 2015 followed by a dry summer reduced the photosynthetic C fixation and resulted in a relatively high annual NEE, but this was counterbalanced by a low biomass production and thus a low harvest export. Surprisingly, the respiration of soil organic matter did not react significantly to the inter-annual difference of weather conditions. The rather constant mineralisation rates are probably due to the highly degraded recalcitrant peat material, and that in the warm season the amount of peat exposed to oxygen (and thus prone to mineralization) is not limited by the groundwater level but rather by the shallow peat layer depth. Whether our results generally apply to drained organic soils under long-term agricultural use with shallow peat layers needs to be tested at other similar sites.

Declaration of Competing Interest

The authors declare that they have no known competing financial interests or personal relationships that could have appeared to influence the work reported in this paper.

Acknowledgements

We gratefully acknowledge the financial support by the Federal Office for the Environment (Vertrags-Nr.: 13.0057.KP / M344-1280). A great thanks to Markus Jocher for technical support, Renato Rüfenacht and Simon Tresch for their help in the field, and Karl Voglmeier for his support on R programming and statistical evaluation. We are grateful to Kristy Klein for language editing and critical comments on the manuscript.

References

- Allakhverdiev, S.I., Kreslavski, V.D., Klimov, V.V., Los, D.A., Carpentier, R., Mohanty, P., 2008. Heat stress: an overview of molecular responses in photosynthesis. *Photosynth. Res.* 98, 541–550.
- Alm, J., Schulman, L., Walden, J., Nykänen, H., Martikainen, P.J., Silvola, J., 1999. Carbon Balance of a boreal bog during a year with exceptionally dry summer. *Ecology* 80, 161–174.
- Ammann, C., Flechard, C.R., Leifeld, J., Neftel, A., Fuhrer, J., 2007. The carbon budget of newly established temperate grassland depends on management intensity. *Agric. Ecosyst. Environ.* 121, 5–20.
- Aslan-Sungur, G., Lee, X., Evrendilek, F., Karakaya, N., 2016. Large interannual variability in net ecosystem carbon dioxide exchange of a disturbed temperate peatland. *Sci. Total Environ.* 554–555, 192–202.
- Aubinet, M., Grelle, A., Ibrom, A., Rannik, Ü., Moncrieff, J., Foken, T., Kowalski, A.S., Martin, P.H., Berbigier, P., Bernhofer, Ch., Clement, R., Elbers, J., Granier, A., Grünwald, T., Morgenstern, K., Pilegaard, K., Rebmann, C., Snijders, W., Valentini, R., Vesala, T., 1999. Estimates of the annual net carbon and water exchange of forests: the EUROFLUX methodology. *Adv. Ecol. Res.* 113–175. Elsevier.
- Bader, C., Müller, M., Schulin, R., Leifeld, J., 2017. Amount and stability of recent and aged plant residues in degrading peatland soils. *Soil Biol. Biochem.* 109, 167–175.
- Beyer, C., Liebersbach, H., Höper, H., 2015. Multiyear greenhouse gas flux measurements on a temperate fen soil used for cropland or grassland. *J. Plant Nutr. Soil Sci.* 178, 99–111.
- Bubier, J., Crill, P., Mosedale, A., Frolking, S., Linder, E., 2003a. Peatland responses to varying interannual moisture conditions as measured by automatic CO₂ chambers: Peatland responses to interannual moisture. *Global Biogeochem. Cycles* 17 (2), 1066.
- Bubier, J.L., Bhatia, G., Moore, T.R., Roulet, N.T., Lafleur, P.M., 2003b. Spatial and temporal variability in growing-season net ecosystem carbon dioxide exchange at a large Peatland in Ontario, Canada. *Ecosystems* 6, 353–367.
- Cai, T., Flanagan, L.B., Syed, K.H., 2010. Warmer and drier conditions stimulate respiration more than photosynthesis in a boreal peatland ecosystem: analysis of automatic chambers and eddy covariance measurements. *Plant Cell Environ.* 33, 394–407.
- Carter, M.R., Gregorich, E.G., 2006. Soil sampling and method of analysis, second ed. *Can. J. Soil Sci.*
- Deventer, M.J., Griffis, T.J., Roman, D.T., Kolka, R.K., Wood, J.D., Erickson, M., Baker, J. M., Millet, D.B., 2019. Error characterization of methane fluxes and budgets derived from a long-term comparison of open- and closed-path eddy covariance systems. *Agric. For. Meteorol.* 278, 107638.
- Drollinger, S., Maier, A., Glatzel, S., 2019. Interannual and seasonal variability in carbon dioxide and methane fluxes of a pine peat bog in the Eastern Alps, Austria. *Agric. Forest Meteorol.* 275, 69–78.
- EddyPro® Version 6.2.1 [Computer software], 2016. Infrastructure for Measurements of the European Carbon Cycle Consortium. Lincoln, NE. LICOR, Inc.
- Evans, C.D., Renou-Wilson, F., Strack, M., 2016. The role of waterborne carbon in the greenhouse gas balance of drained and re-wetted peatlands. *Aquat. Sci.* 78, 573–590.
- Evans, C., Artz, R., Moxley, J., Smyth, M-A., Taylor, E., Archer, N., Burden, A., Williamson, J., Donnelly, D., Thomson, A., Buys, G., Malcolm, H., Wilson, D., Renou-Wilson, F., Potts, J., 2017. Implementation of an Emission Inventory for UK Peatlands. Report to the Department for Business, Energy and Industrial Strategy, Centre for Ecology and Hydrology, Bangor, p. 88.
- Felber, R., Neftel, A., Ammann, C., 2016. Discerning the cows from the pasture: quantifying and partitioning the NEE of a grazed pasture using animal position data. *Agric. For. Meteorol.* 216, 37–47.
- FOEN, 2020. Switzerland's Greenhouse Gas Inventory 1990–2018: National inventory report 2017. Federal Office for the Environment, Bern.
- Ferré, M., Müller, A., Leifeld, J., Bader, C., Müller, M., Engel, S., Wichmann, S., 2019. Sustainable management of cultivated peatlands in Switzerland: insights, challenges, and opportunities. *Land Use Policy* 87, 104019.
- Flanagan, L.B., Syed, K.H., 2011. Stimulation of both photosynthesis and respiration in response to warmer and drier conditions in a boreal peatland ecosystem: Peatland carbon dioxide exchange. *Global Change Biol.* 17, 2271–2287.
- Frank, S., Tiemeyer, B., Bechtold, M., Lücke, A., Bol, R., 2017. Effect of past peat cultivation practices on present dynamics of dissolved organic carbon. *Sci. Total Environ.* 574, 1243–1253.
- Frolking, S., Talbot, J., Jones, M.C., Treat, C.C., Kauffman, J.B., Tuittila, E.-S., Roulet, N., 2011. Peatlands in the Earth's 21st century climate system. *Environ. Rev.* 19, 371–396.
- Gash, J.H.C., Culf, A.D., 1996. Applying a linear detrend to eddy correlation data in realtime. *Boundary Layer Meteorol.* 79, 301–306.

- Gibberd, M., 2001. Waterlogging tolerance among a diverse range of trifolium accessions is related to root porosity, lateral root formation and "aerotropic rooting. *Ann. Bot. (Lond.)* 88, 579–589.
- Glatzel, S., Lemke, S., Gerold, G., 2006. Short-term effects of an exceptionally hot and dry summer on decomposition of surface peat in a restored temperate bog. *Eur. J. Soil Biol.* 42, 219–229.
- Goulden, M.L., Munger, J.W., Fan, S.-M., Daube, B.C., Wofsy, S.C., 1996. Measurements of carbon sequestration by long-term eddy covariance: methods and a critical evaluation of accuracy. *Global Change Biol.* 2, 169–182.
- Griffis, T.J., Rouse, W.R., Waddington, J.M., 2000. Interannual variability of net ecosystem CO₂ exchange at a subarctic fen. *Global Biogeochem. Cycles* 14, 1109–1121.
- Hahn-Schöfl, M., Zak, D., Minke, M., Gelbrecht, J., Augustin, J., Freibauer, A., 2011. Organic sediment formed during inundation of a degraded fen grassland emits large fluxes of CH₄ and CO₂. *Biogeochemistry* 8, 1539–1550.
- Han, G., Xing, Q., Yu, J., Luo, Y., Li, D., Yang, L., Wang, G., Mao, P., Xie, B., Mikle, N., 2014. Agricultural reclamation effects on ecosystem CO₂ exchange of a coastal wetland in the Yellow River Delta. *Agric. Ecosyst. Environ.* 196, 187–198.
- IPCC, 2014. 2013 Supplement to the 2006 IPCC Guidelines for National Greenhouse Gas Inventories (Chap. 2). Wetlands. IPCC, Switzerland.
- Jérôme, E., Beckers, Y., Bodson, B., Heinesch, B., Moureaux, C., Aubinet, M., 2014. Impact of grazing on carbon dioxide exchanges in an intensively managed Belgian grassland. *Agric. Ecosyst. Environ.* 194, 7–16.
- Joosten, H., Clarke, D., 2002. Wise Use of Mires and Peatlands: Background and Principles Including a Framework for Decision-Making. International Peat Society. International Mire Conservation Group, Saarijärvi, Finland.
- Jungkunst, H.F., Flessa, H., Scherber, C., Fiedler, S., 2008. Groundwater level controls CO₂, N₂O and CH₄ fluxes of three different hydromorphic soil types of a temperate forest ecosystem. *Soil Biol. Biochem.* 40, 2047–2054.
- Keller, F., Fuhrer, J., 2004. Die Landwirtschaft und der Hitzesommer 2003. *Agrarforschung* 11 (9), 403–410, 2004.
- Knorr, K.-H., Oosterwoud, M.R., Blodau, C., 2008. Experimental drought alters rates of soil respiration and methanogenesis but not carbon exchange in soil of a temperate fen. *Soil Biol. Biochem.* 40, 1781–1791.
- Kormann, R., Meixner, F.X., 2001. An analytical footprint model for non-neutral stratification. *Boundary Layer Meteorol.* 99, 207–224.
- Krüger, J.P., Leifeld, J., Glatzel, S., Szidat, S., Alewell, C., 2015. Biogeochemical indicators of peatland degradation – a case study of a temperate bog in northern Germany. *Biogeochemistry* 12, 2861–2871.
- Kuhry, P., Vitt, D.H., 1996. Fossil Carbon/nitrogen ratios as a measure of peat decomposition. *Ecology* 77, 271–275.
- Lafleur, P.M., Roulet, N.T., Bubier, J.L., Frolking, S., Moore, T.R., 2003. Interannual variability in the peatland-atmosphere carbon dioxide exchange at an ombrotrophic bog: Carbon balance at an ombrotrophic bog. *Global Biogeochem. Cycles* 17, 1036.
- Leifeld, J., 2018. Distribution of nitrous oxide emissions from managed organic soils under different land uses estimated by the peat C/N ratio to improve national GHG inventories. *Sci. Total Environ.* 631–632, 23–26.
- Leifeld, J., Ammann, C., Neftel, A., Fuhrer, J., 2011. A comparison of repeated soil inventory and carbon flux budget to detect soil carbon stock changes after conversion from cropland to grasslands. *Global Change Biol.* 17, 3366–3375.
- Leifeld, J., Menichetti, L., 2018. The underappreciated potential of peatlands in global climate change mitigation strategies. *Nat. Commun.* 9, 1071.
- Leifeld, J., Steffens, M., Galego-Sala, A., 2012. Sensitivity of peatland carbon loss to organic matter quality: Peat quality and carbon loss. *Geophys. Res. Lett.* 39, L14704.
- Lutz, E., 2016. Vergleich von entwässerten Flachmoorböden unter *Miscanthus x giganteus* und extensiver Mahdweise im Schweizer Seeland in Cressier. Bachelorthesis University of Basel, Switzerland.
- Maljanen, M., Sigurdsson, B.D., Guðmundsson, J., Óskarsson, H., Huttunen, J.T., Martikainen, P.J., 2010. Greenhouse gas balances of managed peatlands in the Nordic countries – present knowledge and gaps. *Biogeochemistry* 7, 2711–2738.
- Moncrieff, J.B., Massheder, J.M., de Bruin, H., Elbers, J., Friborg, T., Heusinkveld, B., Kabat, P., Scott, S., Soegaard, H., Verhoef, A., 1997. A system to measure surface fluxes of momentum, sensible heat, water vapour and carbon dioxide. *J. Hydrol.* 188–189, 589–611.
- Mauder, Matthias, Foken, Thomas, 2011. Documentation and Instruction Manual of the Eddy Covariance Software Package TK2. Arbeitsergebnisse, Universität Bayreuth, Abteilung Mikrometeorologie, ISSN 1614-8916 46. <https://doi.org/10.5194/bg-5-451-2008>.
- Moncrieff, J.B., Clement, R., Finnigan, J., Meyers, T., 2004. Averaging, detrending and filtering of eddy covariance time series. In: Lee, X., Massman, W.J., Law, B.E. (Eds.), *Dordrecht Handbook of Micrometeorology: a Guide for Surface Flux Measurements*. Kluwer Academic, pp. 7–31.
- Myhre, G., Shindell, D., Bréon, F., Collins, W., Fuglested, J., Huang, J., Koch, D., Lamarque, J., Lee, G., Mendoza, B., Anthropogenic and Natural Radiative Forcing, *Climate Change*, 2013. The physical science basis. In: Contribution of Working Group I to the Fifth Assessment Report of the Intergovernmental Panel on Climate Change. Cambridge, 2013. Cambridge University Press, pp. 659–740.
- Peacock, M., Gauci, V., Baird, A.J., Burden, A., Chapman, P.J., Cumming, A., Evans, J.G., Grayson, R.P., Holden, J., Kaduk, J., Morrison, R., Page, S., Pan, G., Ridley, L.M., Williamson, J., Worrall, F., Evans, C.D., 2019. The full carbon balance of a rewetted cropland fen and a conservation-managed fen. *Agric. Ecosyst. Environ.* 269, 1–12.
- Poyda, A., Reinsch, T., Kluß, C., Loges, R., Taube, F., 2016. Greenhouse gas emissions from fen soils used for forage production in northern Germany. *Biogeochemistry* 13, 5221–5244.
- Reichstein, M., Ciais, P., Papale, D., Valentini, R., Running, S., Viovy, N., Cramer, W., Granier, A., Ogée, J., Allard, V., Aubinet, M., Bernhofer, Chr., Buchmann, N., Carrara, A., Grünwald, T., Heimann, M., Heinesch, B., Knohl, A., Kutsch, W., Loustau, D., Manca, G., Matteucci, G., Miglietta, F., Ourcival, J.M., Pilegaard, K., Pumpanen, J., Rambal, S., Schaphoff, S., Seufert, G., Soussana, J.-F., Sanz, M.-J., Vesala, T., Zhao, M., 2007. Reduction of ecosystem productivity and respiration during the European summer 2003 climate anomaly: a joint flux tower, remote sensing and modelling analysis. *Global Change Biol.* 13, 634–651.
- Reichstein, M., Falge, E., Baldocchi, D., Papale, D., Aubinet, M., Berbigier, P., Bernhofer, C., Buchmann, N., Gilmanov, T., Granier, A., Grunwald, T., Havrankova, K., Ivesniemi, H., Janous, D., Knohl, A., Laurila, T., Lohila, A., Loustau, D., Matteucci, G., Meyers, T., Miglietta, F., Ourcival, J.-M., Pumpanen, J., Rambal, S., Rotenberg, E., Sanz, M., Tenhunen, J., Seufert, G., Vaccari, F., Vesala, T., Yakir, D., Valentini, R., 2005. On the separation of net ecosystem exchange into assimilation and ecosystem respiration: review and improved algorithm. *Global Change Biol.* 11, 1424–1439.
- Renou-Wilson, F., Müller, C., Moser, G., Wilson, D., 2016. To graze or not to graze? Four years greenhouse gas balances and vegetation composition from a drained and a rewetted organic soil under grassland. *Agric. Ecosyst. Environ.* 222, 156–170.
- Sangok, F.E., Maie, N., Melling, L., Watanabe, A., 2017. Evaluation on the decomposability of tropical forest peat soils after conversion to an oil palm plantation. *Sci. Total Environ.* 587–588, 381–388.
- Säurich, A., Tiemeyer, B., Dettmann, U., Don, A., 2019. How do sand addition, soil moisture and nutrient status influence greenhouse gas fluxes from drained organic soils? *Soil Biol. Biochem.* 135, 71–84.
- Signarbieux, C., Feller, U., 2012. Effects of an extended drought period on physiological properties of grassland species in the field. *J. Plant Res.* 125, 251–261.
- Sjögersten, S., Caut, S., Daniell, T.J., Jurd, A.P.S., O'Sullivan, O.S., Stapleton, C.S., Titman, J.J., 2016. Organic matter chemistry controls greenhouse gas emissions from permafrost peatlands. *Soil Biol. Biochem.* 98, 42–53.
- Smith, K.A., Dobbie, K.E., Ball, B.C., Bakken, L.R., Sitaula, B.K., Hansen, S., Brumme, R., Borken, W., Christensen, S., Priemé, A., Fowler, D., Macdonald, J.A., Skiba, U., Klemmedtsen, L., Kasimir-Klemmedtsen, A., Degorska, A., Orlanski, P., 2000. Oxidation of atmospheric methane in Northern European soils, comparison with other ecosystems, and uncertainties in the global terrestrial sink: Methane oxidation in soils. *Global Change Biol.* 6, 791–803.
- Sundström, E., Magnusson, T., Hånell, B., 2000. Nutrient conditions in drained peatlands along a north-south climatic gradient in Sweden. *Forest Ecol. Manag.* 126, 149–161.
- Tiemeyer, B., Albiac Borraz, E., Augustin, J., Bechtold, M., Beetz, S., Beyer, C., Drösler, M., Eblj, M., Eickenscheidt, T., Fiedler, S., Förster, C., Freibauer, A., Giebel, M., Glatzel, S., Heinichen, J., Hoffmann, M., Höper, H., Jurasinski, G., Leiber-Sauheitl, K., Peichl-Brak, M., Roßkopf, N., Sommer, M., Zeitz, J., 2016. High emissions of greenhouse gases from grasslands on peat and other organic soils. *Global Change Biol.* 22, 4134–4149.
- Tiemeyer, B., Freibauer, A., Borraz, E.A., Augustin, J., Bechtold, M., Beetz, S., Beyer, C., Eblj, M., Eickenscheidt, T., Fiedler, S., Förster, C., Gensior, A., Giebel, M., Glatzel, S., Heinichen, J., Hoffmann, M., Höper, H., Jurasinski, G., Laggner, A., Leiber-Sauheitl, K., Peichl-Brak, M., Drösler, M., 2020. A new methodology for organic soils in national greenhouse gas inventories: Data synthesis, derivation and application. *Ecol. Indic.* 109, 105838.
- Toberman, H., Evans, C.D., Freeman, C., Fenner, N., White, M., Emmett, B.A., Artz, R.R. E., 2008. Summer drought effects upon soil and litter extracellular phenol oxidase activity and soluble carbon release in an upland Calluna heathland. *Soil Biol. Biochem.* 40, 1519–1532.
- Turetsky, M.R., Kotowska, A., Bubier, J., Dise, N.B., Crill, P., Hornibrook, E.R.C., Minkinen, K., Moore, T.R., Myers-Smith, I.H., Nykänen, H., Olefeldt, D., Rinne, J., Saarnio, S., Shurpali, N., Tuittila, E.-S., Waddington, J.M., White, J.R., Wickland, K. P., Wilming, M., 2014. A synthesis of methane emissions from 71 northern, temperate, and subtropical wetlands. *Global Change Biol.* 20, 2183–2197.
- van Eck, W.H.J.M., van de Steeg, H.M., Blom, C.W.P.M., de Kroon, H., 2004. Is tolerance to summer flooding correlated with distribution patterns in river floodplains? A comparative study of 20 terrestrial grassland species. *Oikos* 107, 393–405.
- Vartapetian, B.B., Jackson, M.B., 1997. Plant adaptations to anaerobic stress. *Ann. Bot. (Lond.)* 79, 3–20.
- Vickers, D., Mahrt, L., 1997. Quality control and flux sampling problems for tower and aircraft data. *J. Atmos. Oceanic Technol.* 14, 15.
- Visser, S.A., 1983. Application of Van Krevelen's graphical-statistical method for the study of aquatic humic material. *Environ. Sci. Technol.* 17, 412–417.
- von Buttlar, J., Zscheischler, J., Rammig, A., Sippel, S., Reichstein, M., Knohl, A., Jung, M., Menzer, O., Arain, M.A., Buchmann, N., Cescatti, A., Gianelle, D., Kiely, G., Law, B.E., Magliulo, V., Margolis, H., McCaughey, H., Merbold, L., Migliavacca, M., Montagnani, L., Oechel, W., Pavelka, M., Peichl, M., Rambal, S., Raschi, A., Scott, R. L., Vaccari, F.P., van Gorsel, E., Varlagin, A., Wohlfahrt, G., Mahecha, M.D., 2018. Impacts of droughts and extreme-temperature events on gross primary production and ecosystem respiration: a systematic assessment across ecosystems and climate zones. *Biogeochemistry* 15, 1293–1318.
- Wall, A.M., Campbell, D.I., Mudge, P.L., Schipper, L.A., 2020. Temperate grazed grassland carbon balances for two adjacent paddocks determined separately from one eddy covariance system. *Agric. For. Meteorol.* 287, 107942.
- Webb, E.K., Pearman, G.I., Leuning, R., 1980. Correction of flux measurements for density effects due to heat and water vapour transfer. *Q. J. R. Met. Soc.* 106, 85–100.
- Whiting, G.J., Chanton, J.P., 1992. Plant-dependent CH₄ emission in a subarctic Canadian fen. *Global Biogeochem. Cycles* 6, 225–231.
- WRB, I.W.G., 2014. World Reference Base for Soil Resources 2014. International Soil Classification System for Naming Soils and Creating Legends for Soil Maps. FAO, Rome. World Soil Resources Reports No. 105.
- Wright, A.J., de Kroon, H., Visser, E.J.W., Buchmann, T., Ebeling, A., Eisenhauer, N., Fischer, C., Hildebrandt, A., Ravenek, J., Roscher, C., Weigelt, A., Weisser, W.,

- Voesenek, L.A.C.J., Mommer, L., 2017. Plants are less negatively affected by flooding when growing in species-rich plant communities. *New Phytol.* 213, 645–656.
- Wüst, C., Grünig, A., Leifeld, J., 2015. Locating organic soils for the Swiss greenhouse gas inventory. *Agroscopy Sci.* 26, 1–100, 2015.
- Wutzler, T., Lucas-Moffat, A., Migliavacca, M., Knauer, J., Sickel, K., Šigut, L., Menzer, O., Reichstein, M., 2018. Basic and extensible post-processing of eddy covariance flux data with REddyProc. *Biogeosciences* 15, 5015–5030.